20th Australasian Fluid Mechanics Conference
Perth, Australia
5-8 December 2016

The rheology dependent region in turbulent pipe flow of a Generalised Newtonian fluid

J. Singh, M. Rudman and H. M. Blackburn

Department of Mechanical and Aerospace Engineering
Monash University, Clayton, Victoria 3800, Australia

Abstract

Direct numerical simulations (DNS) of turbulent pipe flow of a Generalised Newtonian (GN) fluid at $Re_\tau = 323$ are analysed to identify the region where GN rheology has the major influence. The flow domain is divided into two parts: in $y^+ < y^+_{up}$ and $y^+ > y^+_{up}$, with the viscosity modelled using a power-law rheology for $y^+ < y^+_{up}$ and a uniform viscosity for $y^+ > y^+_{up}$. Values for y^+_{up} of 35 and 70 are considered. Results show that beyond $y^+ = 70$, the GN rheology has no significant effect on the mean flow or turbulence statistics, and that the effect of GN rheology is confined to the near wall. To understand these results, the turbulent kinetic energy budget of the GN fluid and a Newtonian fluid at the same $Re_\tau = 323$ are compared. The comparison shows that the GN viscosity-dependent terms in the balance either vanish or do not show rheology dependence beyond $y^+ = 70$. The current results imply that in Reynolds averaged Navier–Stokes and Large eddy simulations the GN rheology's effects can be taken care of by modifying the wall functions.

Introduction

Since Reynolds' experiments in 1883, studies of wall bounded turbulent flows have significantly contributed in our understanding of turbulence. Pipe flow is a subset of wall bounded flows which has the characteristic feature of an enclosed geometry, making it easiest to realise in experiments compared to (for example) channel flow [2]. Pipe flow also has direct industrial relevance as pipeline transport is the most common method of transporting fluids in industrial processes. There is a vast literature available on turbulent pipe flow of Newtonian fluids, however, studies that aim to develop understanding in non-Newtonian pipe flow turbulence are far less common.

Non-Newtonian fluids are very common in many industrial applications including mining, polymer processing, waste water treatment etc., as well as in nature. They are different from Newtonian fluids as they do not show a constant viscosity (shear stress divided by shear rate). The viscosity of a non-Newtonian fluid will often depend on shear rate, shear history and in some applications they show partial elastic behaviour. Generalised Newtonian (GN) fluids are a subclass of non-Newtonian fluids for which the viscosity can be defined as a function of the instantaneous shear rate alone. The viscosity of many fluids such as fine particle suspensions, sewage sludge, paint, some polymeric solutions, some bodily fluids such as blood etc. can be well approximated by the GN assumption. These are the fluids of interest here.

The mathematical expression that relates shear stress (or alternatively viscosity) of a GN fluid to the local instantaneous shear rate is termed a rheology model. The parameters of this model are determined from the experimentally measured shear stress versus shear rate curve (i.e. a shear rheogram). In this study we use a power-law rheology model which is a simple and common model that nevertheless expresses the rheology of some materials quite well. The power-law rheology model defines the kinematic fluid viscosity as:

$$\nu = K\dot{\gamma}^{n-1} \tag{1}$$

Here, $\dot{\gamma} = (2s_{ij}s_{ij})^{1/2}$ is the second invariant of the strain rate tensor $\boldsymbol{s}$ and K, n are the model parameters called the consistency and flow index. Equation (1) represents shear-thinning behaviour when $n < 1$ i.e. the fluid viscosity decreases with increasing shear rate. For $n > 1$ shear-thickening behaviour is observed and for $n = 1.0$ a Newtonian rheology is recovered. Shear-thinning behaviour is the most widely observed GN phenomena [3].

For turbulent pipe flow of Newtonian fluids, it is common to split the flow domain into a viscous wall region ($y^+ < 50$) and an outer layer ($y^+ > 50$) [4]. Here, y^+ is the non-dimensional distance from the wall defined using pipe radius R, fluid viscosity ν and friction velocity u_τ as $y^+ = u_\tau R/\nu$. The fluid viscosity is known to be important only in the viscous wall region. However, in the case of a shear-thinning fluid where the fluid viscosity increases with decreasing shear rate (and hence with distance from the wall), the extent of the viscous region is not well known.

DNS is a powerful tool in understanding wall bounded turbulence. In this study we use a powerful feature of DNS, (i.e. the ability model unreal physics), to identify the region where shear-thinning behaviour is important. This is done by running DNS in which shear-thinning rheology is used only in the near-wall region and Newtonian rheology is used away from the wall. The results will show if non-uniform viscosity and viscosity fluctuations away from the wall have any effect on the overall turbulent pipe behaviour, and confirm where they must be considered. This result will have implications for the development of turbulence models suitable for GN fluids in higher Reynolds numbers flows.

Computational Details

Numerical Method

We use the Semtex code [1] which is a spectral element-Fourier DNS code [1] to solve the following governing equations.

$$\partial \boldsymbol{u}/\partial t + \boldsymbol{u}\cdot\boldsymbol{\nabla}\boldsymbol{u} = -\boldsymbol{\nabla}p + \boldsymbol{\nabla}\cdot\boldsymbol{\tau} + \boldsymbol{f}, \quad \text{with} \quad \boldsymbol{\nabla}\cdot\boldsymbol{u} = 0. \tag{2}$$

Here, $\boldsymbol{u}$ is the velocity vector, p, $\boldsymbol{\tau}$ and $\boldsymbol{f}$ are pressure, shear stress tensor and body force, each divided by the fluid density. We will refer to them as pressure, shear stress and body force despite this scaling.. The shear stress $\boldsymbol{\tau}$ is defined using the GN assumption as $\boldsymbol{\tau} = 2\nu(\dot{\gamma})\boldsymbol{S}$.

In the current simulations the pipe is periodic, $10D$ long and discretised with 288 Fourier modes in the axial direction. The pipe cross-section is covered by 297 spectral elements that use 10^{th} order Gauss-Lobatto-Legendre polynomials. Implementation of a pressure gradient in the Fourier direction is implemented via the body force term by setting $f_z = \partial p/\partial z$. The non-uniform viscosity of the non-Newtonian fluid is handled

by decomposing it into a spatially constant ν_{ref} and a spatially varying component $\nu - \nu_{ref}$. The spatially constant component ν_{ref} is treated implicitly whereas $\nu - \nu_{ref}$ is treated explicitly in time. For more details see [1] and [6].

Mesh Spacing and Simulation Parameters

We define the generalised and friction Reynolds numbers as:

$$Re_G = U_b D/\nu_w \quad Re_\tau = u_\tau R/\nu_w \tag{3}$$

Here, D and R are pipe diameter and radius, U_b is the bulk velocity (flow rate per unit area), u_τ is the friction velocity defined as $u_\tau = (\tau_w/\rho)^{1/2}$ where the mean wall shear stress is $\tau_w = (D/4)\partial p/\partial z$. In equation (3) the mean wall viscosity ν_w is chosen as the viscosity scale as suggested in [7]. For a power-law fluid ν_w is easily written as:

$$\nu_w = (K^{1/n}/\rho)(\tau_w)^{1-1/n} \tag{4}$$

The non-dimensional distance from the wall is defined as $y^+ = (R-r)u_\tau/\nu_w$, where r is the radial distance from the pipe centre. In the current simulations ($Re_G = 11000$, $Re_\tau = 323$), the near wall mesh spacing is $\Delta y^+ = 1$ and $\Delta(r\theta)^+ = 7$. A uniform mesh spacing of $\Delta z^+ = 25$ is used in the axial direction.

We consider three cases with decreasing width of the non-Newtonian rheology domain. First we run the simulation where PL rheology is assumed at all y^+ (case *I*). The fluid viscosity is modelled via equation 1 with the model parameters $K = 345.35 \times 10^{-6}$ Pa s^{-n} and $n = 0.6$. In the other two PL cases, we limit the non-Newtonian domain up to $y^+ = y^+_{up}$ (see table 1) and beyond that use a uniform viscosity which is set equal to the mean viscosity observed in case *I* at the same y^+_{up}. An additional simulation is run with Newtonian rheology, i.e. a constant viscosity that is set equal to the mean wall viscosity ν_w in the PL simulations. A fixed axial forcing $f_z = 0.01165$ N m^{-1} is used in all simulations.

Case	y^+_{up}	ν_N/ν_w
I	323	–
II	70	2.6
III	35	2.0
Newt.	–	1

Table 1: Upper limit of the non-Newtonian domain in different cases. The pipe radius is $R^+ = 323$ in wall units. y^+_{up} is the upper limit of the non-Newtonian domain and ν_N is the fixed viscosity used in case *II* and *III* beyond y^+_{up}. The mean wall viscosity is fixed in wall simulations to $\nu_w = 8.33 \times 10^{-5}$ m^{2}s^{-1}.

Results

In this section we compare the results of simulations with restricted non-Newtonian rheology domain (*II* and *III*) with those from the full non-Newtonian simulation *I* to identify the region where the non-Newtonian rheology is important.

Mean Flow and Velocity Fluctuations

Profiles of the mean viscosity are shown in figure 1a, and as set, a uniform viscosity is observed in simulations *II* and *III* for $y^+ > y^+_{up}$. Viscosity profiles below y^+_{up} are indistinguishable from each other. It appears that the mean axial velocity profiles for all three simulations collapse on a single curve (figure 1b). However, a closer look (not shown) shows that the profile of *III* deviates above the others for $y^+ < 30$ and beyond that deviates below. Profiles of the mean axial velocity gradient (figure 1c) for simulation *III* show deviation from the others largely in the viscous sub-layer ($y^+ < 5$). Unlike Newtonian fluids, shear-thinning fluids do not follow the Newtonian law of wall i.e. $U_z^+ = y^+$ in the viscous sub-layer ($\partial U_z^+/\partial y^+ \neq 1$) (see the inset plot in figure 1c). Instead, $\partial U_z^+/\partial y^+$ increases slightly in the viscous sub-layer as the fluid becomes more shear-thinning, with the explanation being complex and tangential to the discussion here. Deviation between the U_z^+ profiles of the PL simulations and the Newtonian log-law is due to shear-thinning as noted in [6, 7].

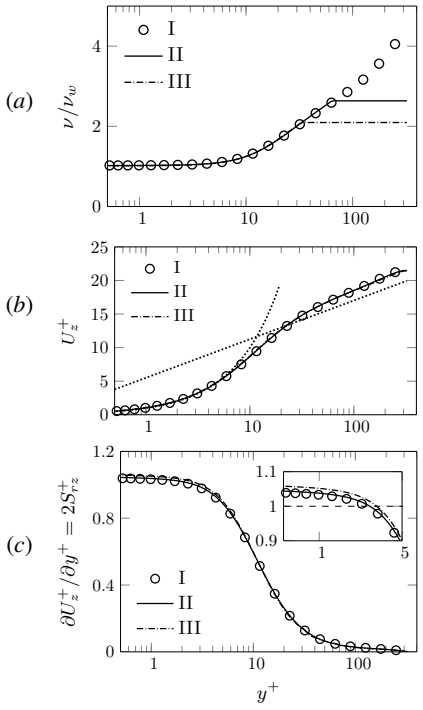

Figure 1: Profiles of (a) the mean viscosity and (b) the mean axial velocity plotted in wall units. Dotted lines in (b) show the classical Newtonian law of wall $U_z^+ = y^+$, $U_z^+ = 2.5 \ln y^+ + 5.5$. The effect of switching the rheology model is negligible on the mean axial velocity profiles.

The effect of restricting PL rheology to the near wall region is seen a little more clearly in the profiles of rms velocity fluctuations (figure 2). The differences between *I* and *II* are very small and seen only in the radial and the azimuthal velocity fluctuations for $y^+ > 70$. In contrast, all velocity fluctuation profiles of *III* clearly deviate from *I*. The axial velocity fluctuation profile starts to deviate in the viscous sub-layer itself but profiles of the other components show deviation only for $y^+ > 20$.

Mean Shear Stress

After using the Reynolds decomposition for velocity $\boldsymbol{v} = \boldsymbol{V} + \boldsymbol{v}'$, strain rate tensor $\boldsymbol{s} = \boldsymbol{S} + \boldsymbol{s}'$, kinematic viscosity $\nu = \bar{\nu} + \nu'$ and pressure $p = P + p'$, the Reynolds averaged Navier–Stokes equation for a GN fluid is written as:

$$\boldsymbol{V} \cdot \boldsymbol{\nabla V} = \boldsymbol{\nabla} P + \boldsymbol{\nabla} \cdot (\boldsymbol{\tau^v} + \boldsymbol{\tau^R} + \boldsymbol{\tau^{fv}}) \tag{5}$$

Here, $\boldsymbol{\tau^v} = 2\nu \boldsymbol{S}$ is the mean viscous stress tensor, $\boldsymbol{\tau^R} = -\overline{\boldsymbol{v'v'}}$ is the Reynolds stress tensor and $\boldsymbol{\tau^{fv}} = 2\overline{\nu' \boldsymbol{s'}}$ is an additional stress term (turbulence viscous stress) which is non-zero only for non-Newtonian fluids. The total mean shear stress $\boldsymbol{\tau}$ is given by the sum of these three components. In the case of a pipe flow, only the rz component of $\boldsymbol{\tau}$ survives and therefore, in the following the subscript rz is dropped for clarity. In a pipe flow, the total

shear stress in the rz direction must be zero at the centreline and τ_w at the wall, hence it is easy to show that $\tau^+ = r/R$ which is independent of the fluid rheology. Therefore, any change in one component leads to change in others.

The mean viscous stress τ^{v^+} and the Reynolds stress τ^{R^+} profiles of *I* and *II* overlap but deviate from those of *III* for $y^+ < 5$ and $y^+ > 30$ (figure 3). The effect of restricting non-Newtonian rheology in simulations *II* and *III* directly affects the turbulence viscous stress τ^{fv^+}. By forcing a Newtonian rheology for $y^+ > y^+_{up}$, we also force $\nu' = 0$ there. Therefore, τ^{fv^+} vanishes for $y^+ > y^+_{up}$ and τ^{v^+}, τ^{R^+} change to keep the total mean shear constant at a given y^+. However, because τ^{fv^+} has already decayed to almost zero by $y^+ = 70$, there are no noticeable differences in the profiles of τ^{v^+} and τ^{R^+} between *I* and *II*.

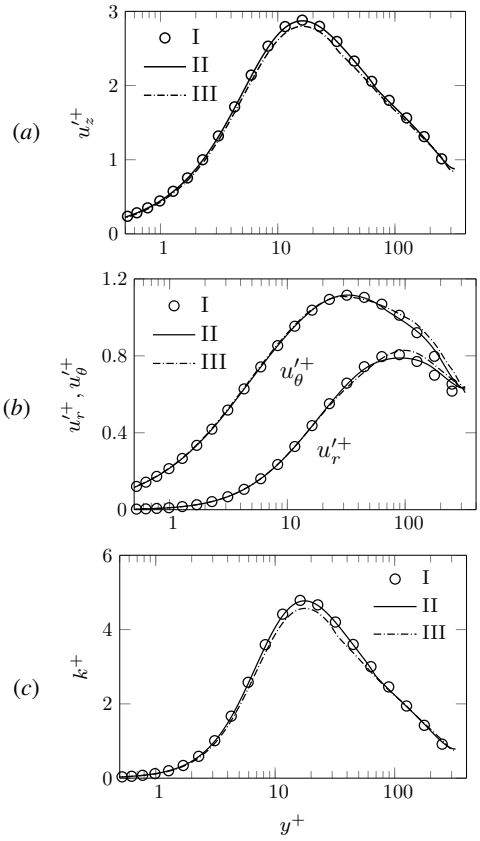

Figure 2: Profiles of the rms velocity fluctuations in the (a) axial direction (b) radial and the azimuthal direction (c) turbulence kinetic energy k. Profiles of *I* and *II* almost overlap each other but deviate from those of *III*.

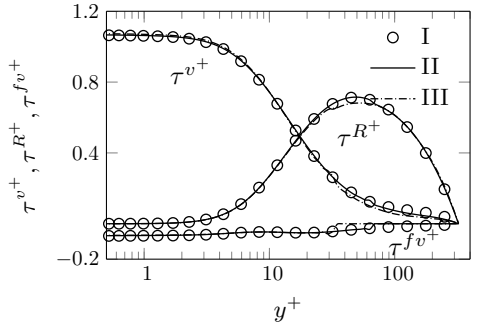

Figure 3: Profiles of the rz component of the mean viscous stress τ^{v^+}, Reynolds stress τ^{R^+} and the turbulent viscous stress τ^{fv^+} plotted in wall units.

<u>Summary</u>

Results presented in this section show that PL viscosity fluctuations for $y^+ > 70$ do not influence the results of the mean axial velocity and velocity fluctuations to any notable extent.

Discussion

In figure 1b, we observed a higher mean axial velocity in *III* compared to *I* and *II* which is due to a lower Reynolds stress τ^{R^+} for *III* as seen in figure 3. The lower τ^{R^+} causes lesser mean flow energy destruction (or turbulence production, discussed later) by τ^{R^+} in *III* compared to others and results in higher mean flow kinetic energy $K = (1/2)U_z^2$ and hence higher U_z in *III* than others.

In order to understand the changes to the turbulence kinetic energy profiles caused by restricting the PL rheology domain (figure 2c), we first compare the turbulence kinetic energy (TKE) budget of a Newtonian and PL fluid (simulation *I*) at $Re_\tau = 323$. After using the Reynolds decomposition (discussed earlier) an equation for TKE $k = (1/2)\overline{u_i' u_i'}$ for a time-stationary turbulent flow is written as:

$$\overbrace{U_j \frac{\partial k}{\partial x_j}}^{1,\mathcal{A}} = \overbrace{-\overline{u_i' u_j'} S_{ij}}^{2,\mathcal{P}} + \left\{ \overbrace{-\frac{\partial \overline{u_i' u_i' u_j'}}{\partial x_j}}^{3,\mathcal{T}} \overbrace{-\frac{\partial \overline{p' u_j'}}{\partial x_j}}^{4,\Pi} + \overbrace{\frac{\partial (2\bar{\nu} \overline{s_{ij}' u_i'})}{\partial x_j}}^{5,\mathcal{D}} \right\}$$
$$\overbrace{-2\bar{\nu} \overline{s_{ij}' s_{ij}'}}^{6,\varepsilon} + \left\{ \overbrace{\frac{\partial (\overline{2\nu' u_i'} S_{ij})}{\partial x_j}}^{7,\xi_{nn}} + \overbrace{\frac{\partial (2\nu' s_{ij}' u_i')}{\partial x_j}}^{8,\mathcal{D}_{nn}} \right\}$$
$$\overbrace{-\overline{2\nu' s_{ij}'} S_{ij}}^{9,\chi_{nn}} \overbrace{-2\overline{\nu' s_{ij}' s_{ij}'}}^{10,\varepsilon_{nn}} \quad (6)$$

Here, terms 1-6 are common for Newtonian and GN fluids but terms 7-10 are non-zero only for GN fluids. In the case of a homogeneous uni-directional pipe flow, term 1, the mean flow advection $\mathcal{A}$ vanishes and the TKE budget is a balance amongst terms 2–10. Turbulence receives energy from the mean flow via term 2 ($\mathcal{P}$, the turbulence production) which is spatially redistributed within the domain by terms 3–5 (i.e. the turbulence transport ($\mathcal{T}$), pressure gradient work (Π) and mean viscous transport ($\mathcal{D}$)). Term 6 (ε, the mean viscous dissipation) represents the destruction of TKE due to the mean viscosity.

In the non-Newtonian terms 7–10, terms 7 (ξ_{nn},the mean shear turbulence transport) and 8 ($\mathcal{D}_{nn}$, the turbulence viscous transport) are again transport terms and these modify the turbulence transport by the Newtonian terms 3–5. Similarly, terms 9 (χ_{nn},the turbulence shear stress–mean strain contraction) and 10 (ε_{nn}, the turbulence viscous dissipation) modify the Newtonian dissipation ε depending on their sign. The modification of TKE the budget by shear-thinning is discussed in [5]. Here, we include only the results of the viscosity dependent terms 5–8.

All viscosity dependent transport terms $\mathcal{D}^+$, ξ^+_{nn} and $\mathcal{D}^+_{nn}$ vanish beyond $y^+ = 30$ and only the dissipation terms survive (figure 4). Although, the Newtonian dissipation ε shows rheology dependence up to $y^+ = 200$, the rheology effect is very small beyond $y^+ = 70$ (figure 4a). For the GN dissipation terms, χ^+_{nn} vanishes and ε^+_{nn} decays to almost zero by $y^+ = 70$. We note that χ^+_{nn} and ε^+_{nn} are positive and therefore, both decrease the total viscous dissipation. The non-Newtonian and Newtonian

dissipation terms when summed together, show rheology dependence only for $y^+ < 70$ (figure 4d).

In simulations *II* and *III*, the (unphysical) mean viscosity for $y^+ > y^+_{up}$ will affect $\mathcal{D}^+$ and ε^+ whereas forcing $\nu' = 0$ will cause the non-Newtonian terms to vanish beyond y^+_{up}. Because by $y^+ = 70$ all viscosity dependent terms except ε^+ decay to almost zero and ε^+ also show little rheology dependence, the TKE budgets for simulations *I* and *II* will agree with each other. In contrast, profiles of the TKE budget terms for *III* are expected to deviate from those of *I* because ε^+ largely depends on the fluid viscosity (and hence rheology) and ε^+_{nn} is still large in the range $30 < y^+ < 70$. Because of the complex interaction between transport terms in the TKE budget, profiles from *III* are not expected to deviate from *I* exactly at the same location where terms 5–8 of *III* show differences from those in *I*.

<u>Summary</u>

Comparison of viscosity dependent TKE budget terms of Newtonian and the PL fluids shows that the PL rheology influences TKE budget via fluid viscosity mainly for $y^+ < 70$.

Conclusions

The current study is a step forward towards understanding pipe flow turbulence of shear-thinning fluids. By exploiting the ability of DNS to model physically impossible situations, the GN rheology dependent region in turbulent pipe flow has been identified. Simulations are run with a restricted GN rheology domain and results show that modifying the fluid rheology beyond $y^+ = 70$ has no significant effect on the mean flow and first-order turbulence profiles. An analysis of the viscosity dependent turbulent kinetic energy budget terms showed that the shear-thinning rheology affects the turbulence kinetic energy budget only for $y^+ < 70$ at $Re_\tau = 323$.

The current study has direct application in rheology characterisation for turbulent flow predictions and in developing turbulence models for RANS and LES of shear-thinning fluids. Results from the current study support the argument presented in [8] that DNS of turbulent pipe flow are very sensitive to the rheology characterisation at high shear rates which are found in the near wall region. Rheology errors at the low shear rates which occur away from the wall are unlikely to affect the overall turbulent flow behaviour. This study also suggests that in RANS and LES based numerical techniques, the effect of shear-thinning could be accommodated by modifying the wall functions.

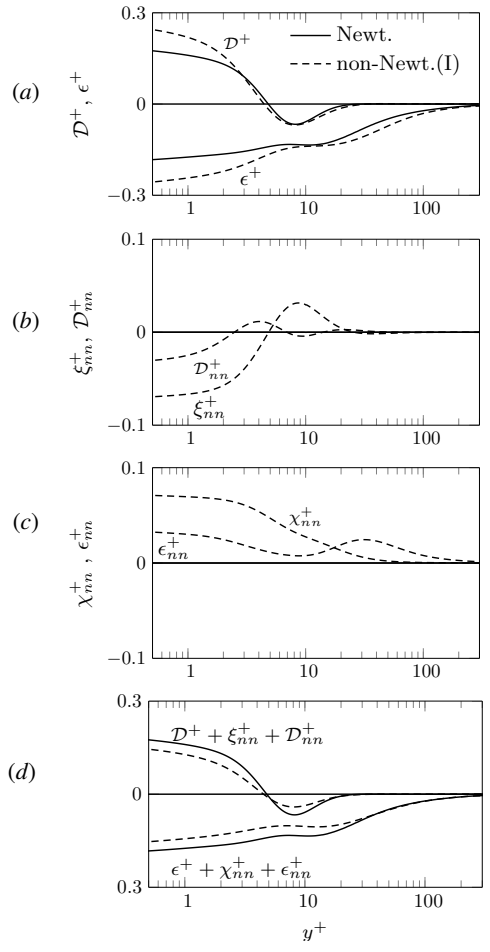

Figure 4: Profiles of (a–c) the viscosity dependent turbulence kinetic energy budget terms 5–8 (see equation (6)) and (d) their sum plotted for a Newtonian (solid line) and PL fluid (dashed lines). The rheology effects are mainly seen in $y^+ < 70$.

Acknowledgements

The authors acknowledge the NCI where these simulations were undertaken on grant D77, and the sponsors of AMIRA P1087 that partially funded the research.

References

[1] Blackburn, H. M. and Sherwin, S. J., Formulation of a galerkin spectral element–fourier method for three-dimensional incompressible flows in cylindrical geometries, *Journal of Computational Physics*, **197**, 2004, 759–778.

[2] El Khoury, G. K., Schlatter, P., Noorani, A., Fischer, P. F., Brethouwer, G. and Johansson, A. V., Direct numerical simulation of turbulent pipe flow at moderately high reynolds numbers, *Flow, Turbulence and Combustion*, **91**, 2013, 475–495.

[3] Khan, S., Royer, J. and Raghavan, S., Aviation fuels with improved fire safety: A proceeding, 1997.

[4] Pope, S. B., *Turbulent flows*, Cambridge university press, 2000.

[5] Rudman, M. and Blackburn, H., Turbulence modification in shear-thinning fluids: preliminary results for power law rheology, in *18th Australian Fluid Mechanics Conference. Launceston, Australia*, 2012.

[6] Rudman, M. and Blackburn, H. M., Direct numerical simulation of turbulent non-Newtonian flow using a spectral element method, *Appl. Math. Mod.*, **30**, 2006, 1229–1248.

[7] Rudman, M., Blackburn, H. M., Graham, L. J. W. and Pullum, L., Turbulent pipe flow of non-Newtonian fluids, *J. Non-Newt. Fluid Mech.*, **118**, 2004, 33–48.

[8] Singh, J., Rudman, M., Blackburn, H., Chryss, A., Pullum, L. and Grahah, L., The importance of rheology characterization in predicting turbulent pipe flow of generalized Newtonian fluids, *J. Non-Newt. Fluid Mech.*, **232**, 2016, 11–21.